J. Mt. Sci. (2023) 20(3): 585-606 e-mail: jms@imde.ac.cn http://jms.imde.ac.cn
https://doi.org/10.1007/s11629-022-7596-y

Original Article

From landslide characterization to nature reserve management: The "Scialimata Grande di Torre Alfina" landslide Geosite (Central Apennines, Italy)

Gianluca TRONTI[1*] https://orcid.org/0000-0002-1445-9299; e-mail: gianluca.tronti@unimi.it

Francesca VERGARI[3] https://orcid.org/0000-0002-5552-0797; e-mail: francesca.vergari@uniroma1.it

Irene Maria BOLLATI[1] https://orcid.org/0000-0002-9195-8008; e-mail: irene.bollati@unimi.it

Filippo BELISARIO[2] https://orcid.org/0009-0003-3711-0158; e-mail: fbelisario@regione.lazio.it

Maurizio DEL MONTE[3] https://orcid.org/0000-0002-9564-3548; e-mail: maurizio.delmonte@uniroma1.it

Manuela PELFINI[1] https://orcid.org/0000-0002-3258-1511; e-mail: manuela.pelfini@unimi.it

Paola FREDI[3] https://orcid.org/0000-0001-7992-7244; e-mail: paola.fredi@fondazione.uniroma1.it

** Corresponding author*

1 Earth Sciences Department "Ardito Desio", University La Statale, Milan 20133, (MI) Italy

2 Monte Rufeno Nature Reserve, Acquapendente 01021, (VT) Italy

3 Earth Sciences Department, University La Sapienza, Rome 00185, (RM) Italy

Citation: Tronti G, Vergari F, Bollati IM, et al. (2023) From landslide characterization to nature reserve management: The "Scialimata Grande di Torre Alfina" landslide Geosite (Central Apennines, Italy). Journal of Mountain Science 20(3). https://doi.org/10.1007/s11629-022-7596-y

Abstract: Italy is characterized by widespread geomorphological instability, among which landslides leave impressive marks on the landscape. Nevertheless, landslide bodies may represent key sites for thematic and educational itineraries, especially in protected areas, where their management becomes an important issue. Our study focuses on the "Monte Rufeno Nature Reserve" (Central Apennines, Italy), where iconic landslides are present. Here, the "Scialimata Grande di Torre Alfina" landslide (SGTA) is listed in the regional Geosite database. This work aims to propose a multiscale procedure for landslide analysis, in terms of both hazard sources but also educational and geoheritage enhancement opportunities in natural reserves. After performing a Landslide Susceptibility conditional Analysis (LSA) for the reserve territory, attention was focused on the SGTA, to define properly its features and morphodynamics. A multi-disciplinary approach was adopted, by applying both remote sensing (UAV structure from motion, Photointerpretation) and field survey (geomorphological and GPS monitoring). From the LSA, based on drainage density, curvature, and slope triggering factors, the road and trail susceptibility maps were derived, as base tools for future risk assessments and trail paths management within the reserve. At the SGTA scale, the monitoring showed a displacement of up to 23 m during the time interval between 2015 and 2018. The landslide dynamics seem to be driven by alternating dry and extremely wet periods; moreover, leaks from the aqueduct in the detachment area and piping effects through clays may have also decreased the substrate cohesion. The SGTA complex influence on the Paglia River valley geometry was also hypothesized, underlining the action of landslide through different spatial scales (on-site and

Received: 06-Jul-2022
Revised: 14-Dec-2022
Accepted: 18-Jan-2023

off-site) and on different environment features (sediment connectivity, hydrology). Finally, the SGTA appears highly representative of the geomorphic dynamics within the Nature Reserve (i.e., scientific value) and it could be classified as an active geosite. Since the site was featured by a tourist trail, adequate management strategies must be adopted, considering the educational value and safety issues.

Keywords: Landslides; Geoheritage; Geosites; Nature reserves management; UAV structure from motion; Landslides conditional analyses

1 Introduction

Gravity processes are very effective in shaping the mountain landscape of the two main mountain ridges of Italy: the Alps and the Apennines. Here, huge mass movements gave place to spectacular landslide deposits, in some cases damming rivers thus inducing, as in other regions of the world, the formation of lakes and interfering with the channel network (Korup et al. 2005). Complex landslides are widespread in the northern Apennines, characterizing the landscape and making this area one of the most hazardous (Bertolini et al. 2017). Where clays prevail, earth and mud flows are widespread, locally called “lame” (Fredi e Lupia Palmieri 2017). Otherwise, all the gravity-related landforms may be considered impacting and scenic features within mountain geoheritage (Coratza & De Waele 2012; Calcaterra, et al. 2014; Forno et al. 2022). Anyway, they induce the generation of hazard and risk scenarios if vulnerable elements are involved. Landslides in the Italian territory are very diverse in terms of bedrock involved, triggering factors (e.g., heavy meteorological events as well as earthquakes), and velocity of movement (e.g., Martino et al. 2020; Forno et al. 2022).

Many geomorphic features related to mass movements are located in protected areas (Brandolini et al. 2013). This implies great attention to their management, especially in areas characterized by tourism, for potential hazards (e.g., Garavaglia et al. 2009), but also because these landforms can be part of the geoheritage. For this reason, in safety conditions, they could become a valid tool, to increase Society’s awareness of potential hazards affecting a territory, especially if characterized by human settlements and infrastructures (e.g., Bollati et al. 2018; Coratza & De Waele 2012).

A huge literature refers to such topic, but little attention is paid to the important role of big landslides in the complex system of ecosystem services, especially in their cultural component (Niculiţă e Mărgărint 2018). This also entails the need for a multidisciplinary approach e.g., (Pelfini & Santilli 2008; Guida et al. 2008; Bollati et al. 2016; Leonelli et al. 2022), to understand landslide systems complexities.

This study focuses on the western part of the Central Italian Apennines – between the Tuscany and Lazio regions – where a horst-and-graben morphology is predominant, due to the extension of the western part of the chain linked to the Tyrrhenian Sea opening. Here the presence of intermontane basins has influenced the drainage network pattern. Another consequence of the extensional dynamic is the development of a series of volcanic complexes (Ciotoli et al. 2003). The interaction between this varied lithological sequence - where a strong caprock covers an easy-erodible bedrock - and the erosive processes shaped peculiar landforms such as badlands, locally called “Calanchi” and “Biancane” (Stark et al. 2020), tabular hills (Margottini, Melelli e Spizzichino 2017), and waterfalls (Fredi e Ciccacci 2017). Moreover, many human settlements are located on the top of mesas, showing spectacular landscapes, increasing the cultural value of the sites, and, thus, attracting several visitors (e.g., Civita di Bagnoregio, Orvieto).

This research has been developed in the context of a Natural Reserve, the "*Monte Rufeno Nature Reserve*" (by now MRNR), located in the Central Italian Apennines, to highlight the potential of mass movements as geoheritage elements at different spatial scales, and provide tools for territorial planning, and hazards analyses for the management of these valued natural resources. The gravity-related processes surely represent hazards and hot spots of geomorphological activity (i.e., geodiversity, environmental gradients), but also peculiar ecological and ecotonal systems, as interruptions of the forest continuity may cause potential evident effects on biotic features (plant and animal species distribution) of the natural environment (Dailling 1994; Shiels and Walker 2013), acting an ecological support role (Bollati et al. 2016).

Within the reserve, great attention has been paid to the huge complex landslide known as the "Scialimata Grande di Torre Alfina" landslide (SGTA), listed in the Regional Geosite Database. It can be considered an “open-air laboratory”, as a good example of an active geomorphosite (Pelfini e Bollati

2014), useful to raise awareness of geomorphological hazards and risks (Coratza & De Waele 2012; Bollati et al. 2013; Pelfini et al. 2016; Forno et al. 2022). Moreover, the activity state of SGTA requires careful management and enhancement, and an accurate risk assessment. Where landslide events affect tourism areas and natural reserves, indeed, their study is even more necessary and important both for management and, as an opportunity, in safety conditions, for education to geomorphological risk. For these reasons, starting in 2004, the SGTA has been objecting to safety measures and tourist trail development. However, in the autumn of 2010, intense and concentrated rainfalls triggered a great retreat of the landslide crown due to the decrease of the slope cohesive forces. Furthermore, a gravity-related displacement of the landslide body, estimated at 12 – 18 meters downvalley was observed. Consequently, a geo-touristic trail was destroyed (Belisario and Romagnoli 2010) and today it testifies to the landslide force, and the rising importance of careful geosite monitoring and management, as emerged in general for active geosites (Bollati et al. 2017b; Diéz-Herrero et al. 2018).

Other studies focused on risk induced by the extreme dynamism affecting these territories (Fantucci & McCord 1995), which, as of the whole Italian Apennines, are characterized by significant susceptibility to slopes instability and a widespread and historical human frequentation (Vergari 2015). The risk assessment methodologies include different approaches and techniques among which Landslides Susceptibility Analyses (LSA), useful to analyze hydrogeological instabilities (Carrara 1995) (Clerici 2006); (Vergari et al. 2011).

This study shows a preliminary LSA in the context of the MRNR, a relatively small Nature Reserve, intending to identify functional tools to manage landslides and their complexity as geoheritage elements that potentially induce risk scenarios in tourism-suited areas. Then attention was focused on the SGTA complex landslide, chosen for its representativeness as an MRNR landslide example, to follow a multi-scalar approach in understanding the gravity processes peculiarities between the MRNR. The aim was to increase the scientific data collection through a multi-disciplinary and multi-techniques approach (UAV structure from motion-*SFM* and photointerpretation, geomorphological surveys combined with multi-temporal monitoring of wooden pins), to define properly its scientific and educational values as geoheritage element, and to propose new elements useful for the valorization of the area, taking in to account the importance of risk management, and mitigation through education.

Hence, according to all the obtained results, the meaning of the SGTA complex landslide as an active geosite and its multiple values as a component of the geoheritage within the framework of the MRNR were discussed.

2 Data and Methods

2.1 Study area

The study area belongs to the "Monte Cetona-Torre Alfina" Mesozoic-Tertiary horst, which is elongated in the NW-SE direction, between Radicofani and Val di Chiana grabens (Tuscany region). According to Bolia et al. (1982), Damiani and Mencarelli (1991) and Damiani (1991), the structural arrangement of the Paglia River drainage basin is the result of the subsequent tectonic events that started from the Upper Oligocene. The outcropping formations are summarized by the following lithological units (Appendix 1):

- Ligurian Units Complex, an allochthonous flyschoid formation with a strong clayey-silty component, overlapping the *Tuscan Complex*, represented in the MRNR area by the *Flysch Tolfetano* unit.
- Tuscan Neogenic Cycle, represented by sedimentary marine deposits, which filled the grabens during the Lower and Middle Pliocene. These units emerge within the MRNR along the major river valley slopes. They are composed mainly of conglomerates, and sandy and clayey marine deposits. Starting from the Middle-Upper Pliocene to the Lower Pleistocene, an uplift and folding phase affected the marine Pliocene deposits in the Radicofani graben. This plastic tectonic style is characterized by anticlines and synclines with N-NW to S-SE axis direction, probably connected to the ascent of the anatectic magma which originates in the Pleistocene the Amiata volcanism (Ciccacci et al. 1988).
- Quaternary Units are mainly represented in the MRNR southern area, where the Vulsino Complex volcanic deposits cover the flysch formations. This volcanic activity refers to a new tectonic extensive phase driven by NE-SW direct faults, which

determines the Vulsino complex collapse and the alkaline potassium manifestations. The Vulsino Complex products are represented by trachibasaltic, leucitic lavas and pyroclastic flows (yellow tuffs), (Amodio et al. 1987). For the aims of this study, these were collected in the analyses by the lithological classes *lava* and *tuff*.

- Finally, the valley floor is characterized by recent alluvial and colluvial deposits (clays, silts, gravels aggregated in the lithological class *alluvial deposits*), related to the intense water-related processes, and by gravity-related deposits (*breccia* lithological class).

The precipitations of the Tyrrhenian side of the Central Apennines, are influenced by the orographic effects along the Monte Cetona - Torre Alfina alignment. The average rainfall value measured in the Falconiera station (Acquapendente, 425m a.s.l.) is above 932 mm/year for the time interval 2004-2021. November results in mean the rainiest month, with an average precipitation of above 153 mm. The maximum rainfalls that occur in consecutive days are more typical in Autumn, from September to November, and are recorded also in years with lower annual rainfalls. These extreme events, preceded by summer dry periods, induce cohesion reduction in clays substrate, promoting gravity processes (Ciccacci et al. 1988; Della Seta et al. 2009; Bollati et al. 2012).

The average annual temperature is 10.3°C. In Autumn (mean of 13.9°C) the temperature is higher than in Spring (mean of 11.8°C) and the thermal excursions averages show the maximum values in summer (mean of 16.1°C) and minimum in winter (mean of 9.1°C), (Appendix 2).

From a phyto-climatic point of view, the average Paglia basin falls within the Temperate Region. The thermotype varies from lower hills, along the valley floor and in the lower slopes, to upper hills on the reliefs and the slope's upper parts. The ombrotype ranges vary from upper subhumid to lower humid in relation to the valley orientation and width (Blasi 1993).

The MRNR was established in 1983 in the Acquapendente area (Central anti-Apennine, Italy) and delimitated from the north: 42°50'4.56"N, 11°53'41.95"E to south: 42°44'15.78"N, 11°55'40.90"E. It is part of the Paglia River hydrographic basin (1187 km^2), in the northern Lazio region and covers an area of 28.9 km^2, characterized by a hilly landscape which reaches the maximum altitude at the "Greppe della Maddalena" (774 m a.s.l.) and the minimum at the Paglia riverbed (235 m a.s.l.), (Fig. 1a). The Paglia River basin (Fig. 1), a tributary of the Tiber River, is characterized by the presence of landforms, which are mainly shaped by gravity and running water processes. Within the MRNR area, a dense forest cover provides a regulating and protective action against running waters. Fluvial erosion represents one of the most effective morphogenetic processes in the examined area. The river valley diversity, at the catchment scale, reflects the lithological variety and the volcanic and neo-tectonic events. The drainage network morphodynamic (in a deepening phase) represents a preparatory and triggering effect for numerous landslides. The "*Scialimata Grande di Torre Alfina*" landslide (by now SGTA) belongs to the Regional Inventory of Geosites of Lazio Region (Belisario 2003; Dir. Reg. Cap. Nat. 2015) as a complex landslide of considerable size (about 0.14 km^2 of area and 3.4 km of perimeter). It has an extremely elongated shape for about 1.5 km from E-SE to W-NW direction, between an altitude of 524 m a.s.l. in the detachment zone and 225 m a.s.l of the Paglia riverbed. The landslide insists on a particularly unstable substrate and shows a complex behaviour that evolves from rotational slide to debris-earth flow. The previous studies (Aleotti et al. 2016) do not allow for establishing the triggering time. Among the main preparatory causes, there is the surface and the underground water circulation, related to the clays fracturing and weathering.

2.2 Landslide susceptibility assessment procedure based on conditional analysis

Landslide Susceptibility (by now LS) maps are useful tools for landscape and hazard management (Sterlacchini 2011).

A conditional analysis at the MRNR scale was carried out to build multivariate LS models, and to produce in a cost-effort efficient way LS maps for the MRNR (Carrara 1995; Clerici 2006; Noti 2018). The analysis was performed in the GIS environment.

The landslide detachment niches (from now DNs) were detected and mapped after photointerpretation and remote sensing analysis, with a dataset dating back to the early 1950s. For this purpose, Google Earth historical series, Orthophotos, Stereo photos, topography and DEM-derived rasters were used (e.g., curvature, hillshade). Landslides belonging to the IFFI landslides national inventory (IFFI 2007) were also considered.

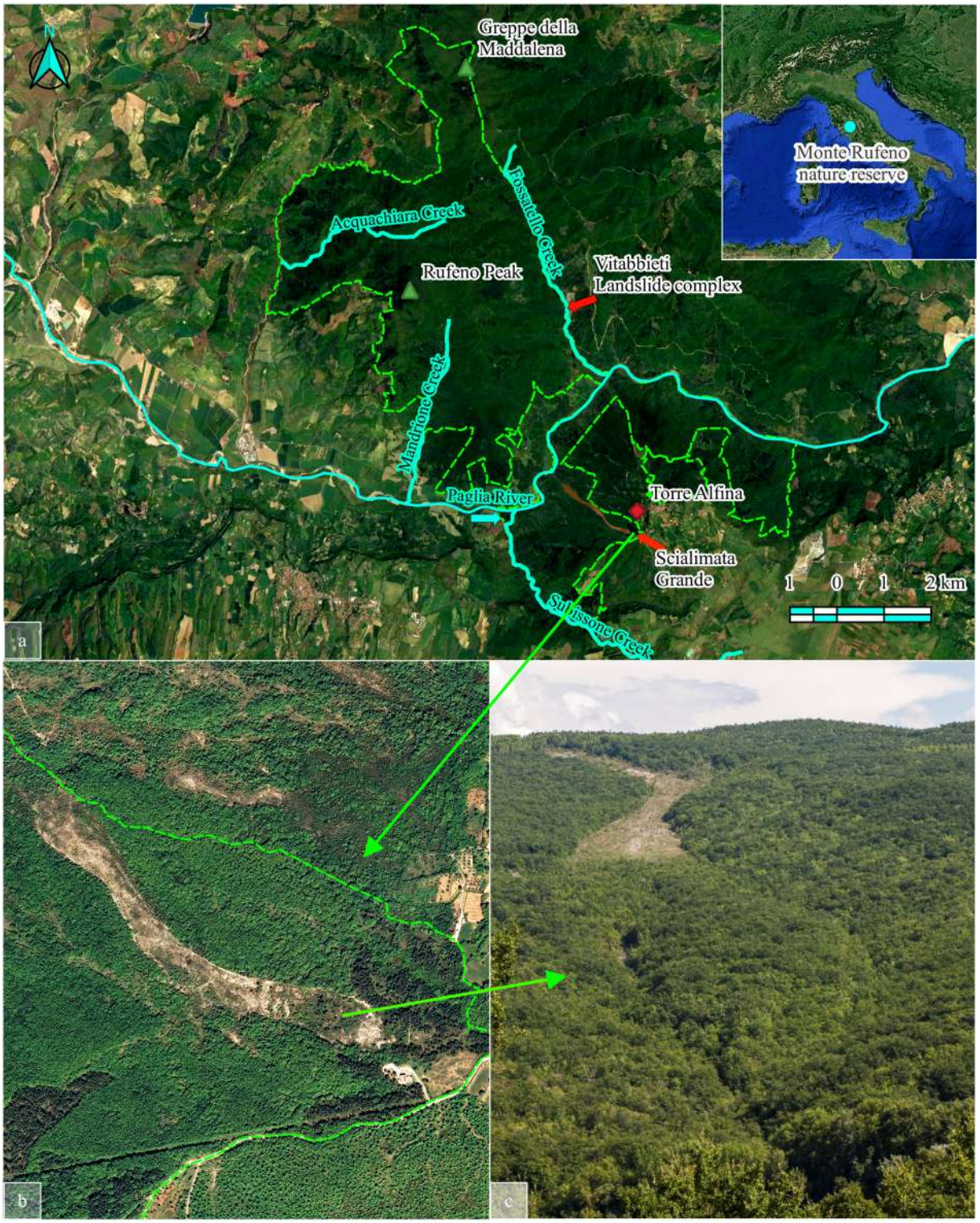

Fig. 1 Study area. (a) Geographical setting; (b) Scialimata Grande nadiral view, the green line highlights the MRNR boundaries; (c) NW view of the Scialimata Grande landslide body. It is evident the presence of vegetation on the landslide lower body.

A total of 7 causal factors were considered for the LS analysis (Appendixes 1, 3) and were derived from two main sources: the national and regional open access vectorial data (Lazio Region Lithology and Land Use maps) and the elevation and hydrographic data of the 1:5000 Lazio topographic map (Lazio Region Open

Data 2002/2003). From the latter, the 5 m resolution Digital Elevation Model was derived by an interpolation process applying the Topo to Raster tool based on the ANUDEM program developed by Hutchinson and Dowling (1991). Starting from this DEM, 4 causal factor maps were derived for the LS analysis: aspect (AS, the orientation of the slope), the amplitude of relief (AR), slope gradient (SL), and curvature (CU). After a reclassification process in a smaller number of classes to minimize the number of small polygons with scarce statistical significance, the factor maps were all transformed into vector data.

Finally, the drainage density factor map (DD) was derived by calculating the cumulative length of stream segments of the drainage network digitized from 1:5000 topographic maps falling within unit areas of 1 km². After an interpolation process of the centroid values of a 1 km² square grid, the drainage density values were reclassified into 4 classes. Similarly, the five classes of the amplitude of the relief map were derived by the interpolation process of the centroids values of a 500 m² grid. The slope, curvature and aspect factor maps were derived by the 20 m resolution aggregate processes and then respectively reclassified into 6, 3 and 4 classes. As regards the vectorial data derived from the land use (LU) and lithology (LI) of the Lazio Region, the factor maps were reclassified both into 6 classes, with a simplification of the starting datasets, according to the similarity in gravity processes responses (Appendix 1).

Many factors could be included in an LS analysis. Often, the selection is made starting from expert-based criteria and observations. In this study, the most representative causal factors were selected through an objective bivariate statistical procedure proposed by Vergari et al. (2011), to reduce at the same time, the small polygons and keep high the model previsioning power. The factor selection procedure involves the evaluation of the Gini index of inequality (Gini 1914) and Lorenz curves, to assess which factors could better explain the past landslides distribution. The Lorenz curves were constructed starting from the intersection of each factor map with the landslide distribution map. Each point on the Lorenz curve represents the cumulative area affected by landslides versus the cumulative portion of the study area characterized by a certain class of a given potential causal factor. The line of perfect equality, the 1:1 red line, represents the theoretical homogeneous distribution of landslides between all the factor classes. The Gini coefficient (G) is graphically represented by the area between the line of perfect equality and the computed Lorenz curve, and can be approximated with trapezoids, calculated using the following formula:

$$G = 1 - \sum_{n=1}^{N} [X_n - X_{n-1})(Y_n + Y_{n-1}) \quad (1)$$

where: n = factor class, N = total number of factor classes, X_n = cumulative portion of the study area characterized by the factor class n, with $X_o = 0$, $X_N = 1$, Y_n = cumulative portion of landslide area falling in the factor class n, with $Y_o = 0$, $Y_N = 1$.

The factors showing a G-value higher than the average value, among all the considered factors, were selected. Moreover, a unique correlation matrix for all the possible pairs of potential factors was computed to reduce the factor's redundancy and to test factors for independency. In fact, the factor selection method, if combined with the study of the correlation between independent variables, does not result in the loss of information, since the discarded factors are often indirectly accounted for by other selected variables.

The overlapping operation between the selected predisposing factors was carried out to identify the vector "Unique Condition Units"- vUCU's for the environmental parameters. vUCU's maps number (N) is defined by the combinations sum of n layers of k factors (binomial Newton coefficient) with k=1, ..., n (Noti 2018):

$$N = \sum_{k=1}^{n} \binom{n}{k} = \sum_{k=1}^{n} \frac{n!}{K!(n-k)!} \quad (2)$$

For each vUCU of each map, the past landslides density, comparable with the landslides occurrence probability, was calculated through the following formula based on conditional analysis:

$$P(L|\text{UCU}) = \frac{\text{Landslide area} \cap \text{vUCUs area}}{(\text{vUCUs area})} \quad (3)$$

For the susceptibility maps production, the landslide density parameter was reclassified in 5 intervals. The intervals were defined to make the average value of the landslide density equal to the central class median (class 3) and to make equal intervals for 1 to 4 classes. The upper limit of the fifth class is instead open. More precisely, by calling Md the mean density, the interval Ci between the classes is expressed as follows:

$$Ci = \left(\frac{2}{5}\right) \text{Md} \quad (4)$$

And the classes are defined: [0, Ci] Very low susceptibility, [Ci, 2Ci] Low susceptibility, [2Ci, 3Ci] Mean susceptibility, [3Ci, 4Ci] High susceptibility, [4Ci, 1] Very high susceptibility.

A five-class classification is a functional compromise between susceptibility distinction and maps readability (Nagarajan et al. 2000; Chung and Fabbri 2003; Ayalew and Yamagishi 2005; Clerici 2006).

The model validation was carried out through a randomized split of the landslides dataset, using 62 landslides for the construction model, and 62 landslides for the validation one (Chung and Fabbri 2003; Remondo et al. 2003; Santacana et al. 2003). The best model evaluation is a comparison of the validation landslide distribution with that predicted through the construction models. For each model, the absolute value of the difference between the percentage areas of the building and validation landslide areas was calculated. This operation was repeated for each of the five susceptibility classes (Noti 2018). The sum of these values for each susceptibility class is defined as model validation error (VE):

$$\mathrm{VE} = \sum_5^1 |(\%\ \mathrm{DN\ building\ area}) - (\%\ \mathrm{DN\ validation\ area})| \quad (5)$$

The index value is inversely proportional to the model goodness. A good model should also be able to distinguish between significantly different landslide densities and provide a spatially detailed forecast: for this reason, a good model should have a great spread or dispersion around the mean density value (Clerici 2006). To quantify the dispersion around the mean value of a distribution, two statistical indices are typically used: the *standard deviation* (SD) and the mean absolute deviation (MD). The first is greatly influenced by the extreme values (often corresponding to small vUCUs with poor statistical value). For this reason, the absolute mean deviation was preferred:

$$\mathrm{MD} = median(|X_i - median\ (X)|) \quad (6)$$

A further index, defined as best model index (BMI) was used to summarize the two previous indices results:

$$\mathrm{BMI} = \frac{\mathrm{MD}}{\mathrm{VE}} \quad (7)$$

The best model choice was also based on the interpretation of prediction and success curves for each susceptibility map (Chung and Fabbri 2003). The success rate curve was obtained from a comparison between the prediction pattern derived from the full landslide dataset with the total landslide distribution. The prediction rate curve, instead, originated by the comparison derived from the split of the original dataset in construction and validation subsets (Fig. 2). The success rate curve measures the goodness of fit, while the prediction rate provides the validation of the prediction. The slope of the prediction rate curve indicates the prediction capacity of the model for a typical random model characterized by a straight prediction line between the two extreme points (0, 0) and (1, 1), (Fig. 2).

Finally, to assess the most critical areas in terms of landslide hazard and touristic fruition, intersect operations between the susceptibility map and the main roads and trails of the MRNR were applied in the GIS environment, developing by this way a useful management tool. In this framework, the SGTA was contextualized respect to the LS map.

2.3 Detailed analyses at the "Scialimata Grande di Torre Alfina" spatial scale

After the elaboration of the LS Maps for the MRNR, the focus was put on the SGTA geosite for a first detailed assessment of dynamic and geomorphological features, using different techniques.

2.3.1 Photogrammetric analysis

Unmanned aerial vehicle-UAV surveys were performed to obtain landslide orthophotos and 3D rendering by the Structure from Motion technique (Yeh et al. 2017; Fugazza et al. 2018; Ramsankaran et al. 2020), and to analyze in detail the morphology of the landslide body (Fig. 3). The UAV surveys were also employed as a support tool to check the punctual monitoring of the landslide dynamic, that was being carried out with wooden pins from 2015 to 2018. The "AeromaX4" quadcopter produced by Microgeo was used for the overflight (Fig. 3b). This can reach 25 minutes of flight and it is equipped with an interchangeable Gimbal that allows it to mount onboard sensors. The drone is also equipped with depth sensors, gyroscopes, and satellite reception. The missions were programmed using the "Mission Planner" software (Fig. 3a). The detection equipment consists of a *Sony α5000 APS-C* camera with 20.1 megapixels, equipped with a 15mm focal length lens. The camera allows video transmission on the 5.8 GHz frequency (FPV-First person view) useful for in-flight monitoring. Two-tone squared tablets were used for the Ground Control Points (by now GCPs) acquisition. The GCPs coordinates were recorded using the Garmin Etrex 20 platform, then manually corrected using the Qgis georeferencing instrument by ground recognizable objects as references.

Four consecutive flights were carried out on 16

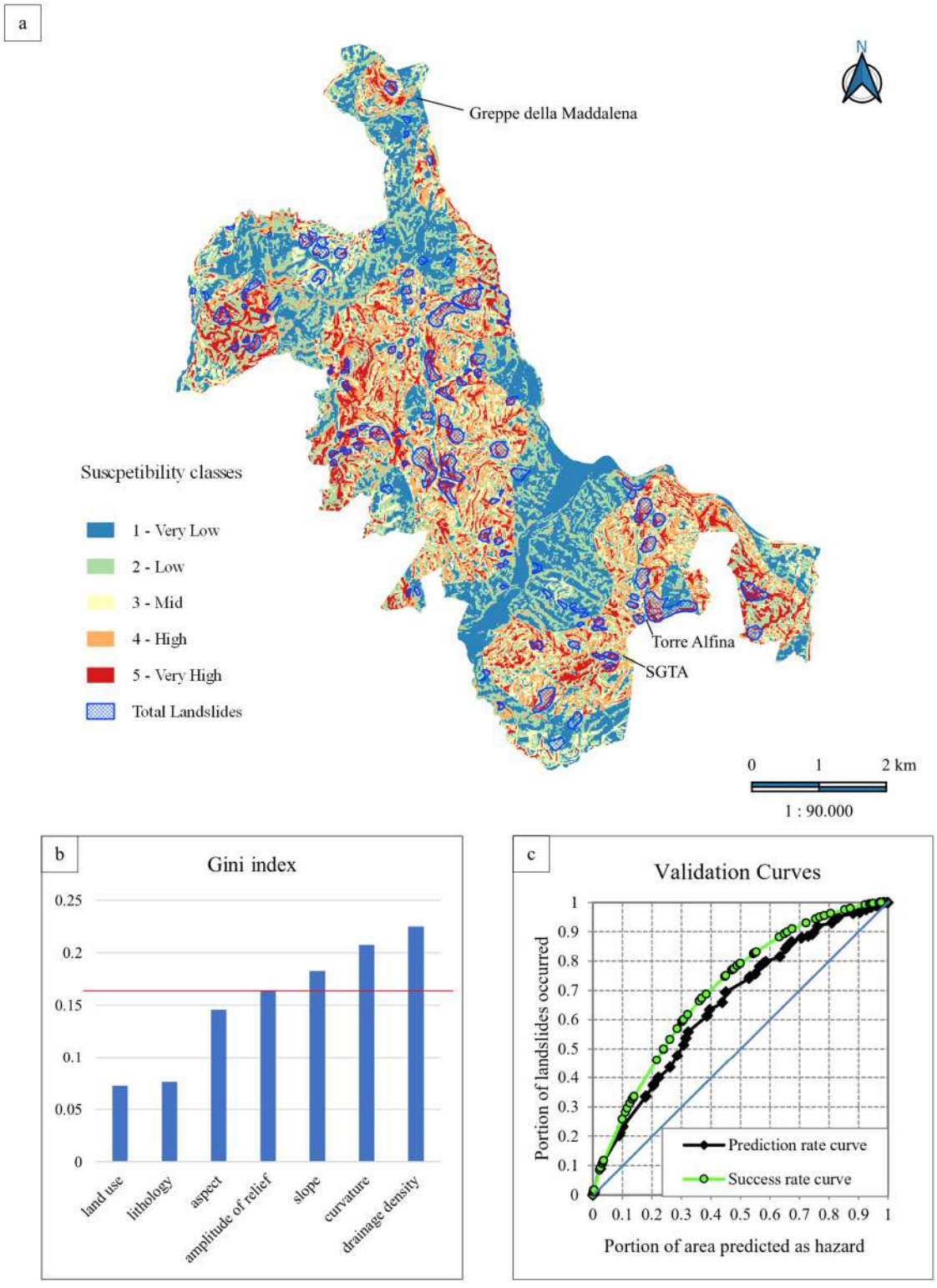

Fig. 2 Results of the landslide susceptibility analysis. (a) Landslide susceptibility map of the MRNR, derived from the susceptibility analyses by using the selected causal factors (DD, SL, CU). (b) Gini index scores for the causal factors (the factors with the highest G values were selected for the susceptibility analysis). (c) Prediction and success rate curves generated using the validation procedure proposed by Chung and Fabbri (2003).

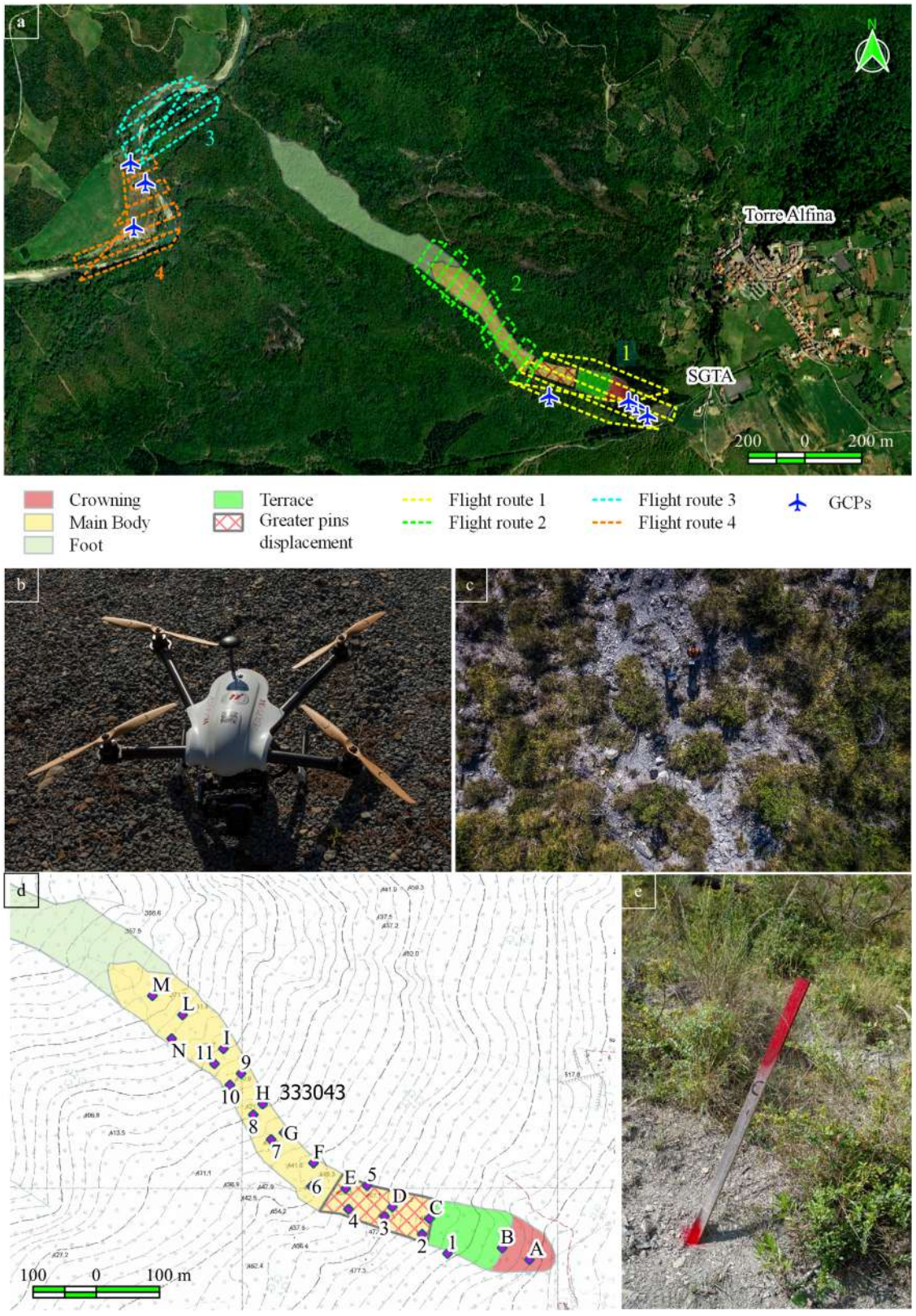

Fig. 3 UAV surveys and punctual monitoring of the landslide dynamic. (a)Flight routes; (b)UAV Microgeo®; (c)nadiral UAV picture crop; (d)starting monitoring pins locations on SGTA; note that the pin 1 has been lost during the monitoring period; (e) Example of the used monitoring pin. In this case the pin c shows an approximate 30° inclination due to the landslide

October 2018. The first two focused on the landslide crown and main body, where the landslide activity is high, and well identified by the scarce vegetation cover. The other one was performed on the Paglia riverbed portion, downstream of the landslide, to evaluate possible influences of the slope instabilities on the riverbed. During the preliminary field campaigns, it was decided to avoid the UAV survey of the lower landslide area, due to the high vegetation cover. Indeed, this can be considered a proxy of relative stability in terms of movements, and a non-neglectable issue for the Sfm technique. The camera was set in time-lapse mode with a shutter interval of 3 seconds. This, combined with the relatively low overflight altitude (about 80 meters) and low fly speed, allowed a high frame overlap (50%-60%) and a theoretical ground resolution of 2 centimetres. The survey atmospheric conditions were good, except for some wind gusts which caused a quality reduction for some frames. In the GCPs positioning, adjustments were made according to the difficult territorial characters. For the georeferencing, the theory provides the location of n control points, with a minimum of 3, proportional to the phenomenon extension and placed in equidistant positions (Yeh et al. 2017; Rossi et al. 2018). This was impossible due to the substrate's high instability and the high vegetation cover. Four GCPs have been placed in the detachment area near "Casale S. Antonio" and 3 GCPs in the Paglia river alluvial area. The images were then processed with "Photoscan professional" software v 1.2 and 1.4. The calculation method uses collinearity equations to establish relationships between images. In addition, the optical camera distortion is corrected in the "Fix calibration" process. The software algorithms reconstruct the point coordinates in the three dimensions, then these are joined to generate polygons and various derivative products (i.e., Sparse points clouds, Dense point clouds, Mesh, DEM, and 3D models (Lucieer et al. 2014).

2.3.2 Geomorphological surveys and landslide monitoring

Geomorphological surveys were carried out on the landslide body and the Paglia river meanders zone immediately downstream, intending to identify gravity and surface running water-related landforms (Ciccacci et al. 1988). For this purpose, ground surveys were adopted and combined with photointerpretation and DEM analyses. Geomorphological sketches were made as a synthesis, according to the ISPRA symbology (Campobasso et al. 2018). Wooden pins were installed on the SGTA body between November 2015 and October 2016 and monitored at least biannually until November 2018. The surveys were carried out with the "Garmin GPSmap 64s" terminals, whose position error was compatible with the magnitude of the observed pins displacements (i.e., about 10 meters/year order). The observed displacements, indeed, exceed the error threshold and allows us to assess a first preliminary description of the landslide movements. Pins positions were sampled in consecutive sessions, and the displacement in meters (Δm) and relative direction were measured. The total displacement ($\Delta Tot.$), the sum of the single displacements, and the displacement between the first and last sampled position and relative direction were then calculated (ΔR). A cross-checking was made with Google Earth historical series function, after which a multitemporal analysis of the most considerable displacements was performed.

The 2015-2018 landslide monitoring results were finally compared to the meteorological records. Rainfall time series were collected starting from the Falconiera meteorological station (450 m a.s.l.), from 2004 to 2021, reporting the monthly rainfalls (Arsial 2018).

3 Results

3.1 Susceptibility maps of the MRNR

The landslide detachment niches (*DN*) inventory of the reserve resulted in a total of 124 polygons. The preliminary bivariate analysis resulted in the selection of the three factors with the highest Gini index (thus resulting as the most discriminant in predicting the landslide niche distribution): DD, SL and CU (Appendix 4). Among these factors, the correlation index shows low correlation values, thus independence among factors is ensured and redundant information is avoided. The resulting susceptibility map and its validation are shown in Fig. 2. The drainage density shows the best Gini index, followed by the curvature and slope factors (Fig. 2b). In contrast, Lithology and Land Use factors commonly used in susceptibility analyses, result here of poor importance, showing the lowest Gini indexes. The amplitude of relief, above the mean for the Gini index, was excluded to reduce the small UCUs and for its similarity in terms of environmental information with the slope parameter. In detail:

- Land Use (LU) - The greatest portion of the MRNR falls under the “Forest” unit (90.5% of the study area) which contains the largest landslide cover (88.4%). “Shrubby and/or herbaceous vegetation areas” unit, despite having a modest surface area (5.14%), is characterized by the presence of a relatively high landslide (10.1%). This is probably explainable by the landslide feedback effect which is responsible for the renewal of the ecological series and a vegetation return towards the pioneer stages. The factor was discarded since the landslides are widespread on the most frequent classes of this factor, being this last non-distinctive for susceptibility classification (as well quantified by the G index).
- Lithological units (LI) - Most of the area falls within the "Flysch Tolfetano" unit (91% of the study area) which is characterized by poor resistance and cohesion. For this reason, most of the landslides (95%) fall within this class. The clear prevalence of a single unit also for this latter causal factor, makes it not useful in the LS models.
- Aspect (AS) - Much of the MRNR area is exposed westward (40%) also showing a great landslides cover (30%). The same slope orientation characterizes also important complex landslides within the reserve as the SGTA. The East exposition (28%) shows the higher landslides cover (39%), probably due to wetter conditions, that in clays substrate could represent an important preparatory factor.
- Amplitude of relief (AR) - Highest values are found where faults and contacts between volcanic and flysches lithologies are present and in correspondence with the river’s greater incisions. The lowest values are found along the Paglia river deposits and in correspondence with the sub-horizontal surfaces of the Vulsini pyroclastic plateaus. The most diffuse classes are intermediate III (38%) and IV (29%), which also show the highest portion of total landslides cover (43% and 36%). The highest energy class V (4%) shows the maximum landslide density.
- Slope (SL) - As in the previous case, areas showing intermediate classes of Slope have the highest frequency of landslides, thus corroborating the importance of homogeneous lithologies in shaping the MRNR hilly landscape. Landslide cover has an approximately Gaussian distribution; in fact, the most widespread classes are the intermediate ones (III, 37% and IV, 32%) show the highest portion of the landslides cover (31% and 36%), being the most diffuse classes. As for the previous factor, the highest slope class V (12% of the total study area) shows the maximum landslide density.
- Curvature (CU) - This factor shows a prevalence of landslides cover (58% of the total detachment areas) for concave areas (39% of the total study area). A simple explanation lies in the high transformation that landslides operate on the landscape. The detachment zones generally show a concave area where sediment depletion is common and directed downvalley, where, in opposition, convex zones can witness the presence of deposit areas.
- Drainage density (DD) - The highest LS class falls in the areas characterized by low and intermediate values of drainage density, despite what is expected. The DNs are generally clustered in the headwaters, where slope processes prevail over processes related to channelled water. This could be explained by the piping phenomenon that characterizes these substrates and that can predispose the slopes to landslides, even if do not provide evidence on the surface, apart from those revealed in specific cases by tilted vegetation (Bollati et al. 2012). This hypothesis would be consistent with the hydrological characteristics of the Flysch formations which characterize most of the MRNR. The clays that compose it, indeed, show a deep alteration of the geotechnical characteristics and permeability, due to the high fracturing and cracking degree (Ciccacci et al. 1988). For these reasons, the drainage density could reflect the importance of underground water flows as a triggering factor. Moreover, this factor can provide an indirect assessment of other environmental parameters such as the outcrop’s erodibility, the tectonic and fracturing effects, the vegetation cover, the slope, the roughness, the slope length, and the annual average rainfall in a drainage basin (Vergari et al. 2011).

Finally, it is interesting to note that the southern area of the MRNR, to which the SGTA belongs, is among those with the highest LS values.

Two other susceptibility maps were derived and attached to this work as final products from the intersect operations between the susceptibility map and the road and trail networks. The road network landslide susceptibility map (Appendix 5) can be a useful tool to assess the landslide risk among the main roads of the MRNR. 10% of the road network falls in the fifth (the highest) susceptibility class, and 18% in the fourth, for a total of 28% of roads characterized by

a high landslide susceptibility. The analysis of the trail network landslide susceptibility (Appendix 6) shows that 12.3% of the trails fall in the fifth and 14.6% in the fourth class, for approximately 27% of trails characterized by a high landslide susceptibility. In this case, the intersect allows us to compare the trail feature with the susceptibility class. It is interesting to highlight the presence of high susceptibility in 2.3% of trails classified as touristic: part of the "Sentiero dei Briganti" and the "Sentiero natura Felceto" in the northern MRNR, and of the "Sentiero del Fiore "in the southern MRNR.

3.2 Detailed analyses of the "Scialimata Grande di Torre Alfina" landslide

3.2.1 UAV-image-based geomorphological analysis

After the UAV surveys carried out in October 2018 and the subsequent data processing, the following objects were obtained:

• 3D textured model of the non-vegetated SGTA portion, obtained from the Sparse Cloud-derived Mesh.

• Orthophotos of the non-vegetated SGTA portion, obtained from the textured Mesh, with a resolution of about 800 megapixels.

• 3D textured model of the Paglia River Meanders area, obtained from the Dense Cloud-derived Mesh.

• Digital surface model (DSM) of the Paglia River Meanders area, created from the Mesh.

• Orthophotos of the Paglia River meanders taken from the Digital Surface Model DSM because the Mesh tended to oversize the tree's height.

These products were used for photo interpretation, for geomorphological survey operations, to check the monitoring pins' positions and as bases on the thematic maps and geomorphological sketches (Fig. 3c; Fig. 4a, Fig. 5a, 5b; Appendix 7a).

Previous studies do not allow for assessing the first triggering time of the SGTA (Aleotti et al. 2016), however, several local witnesses suggest an age of at least 60 years. At the scale of the SGTA landslide, the morphology is extremely chaotic. It is characterized by a large concave area towards the slope and an equally large convex area near the Paglia River. Here, the gullies development has established drainage paths within and adjacent to the landslide (Fig. 4a; Appendix 7a). The main crown scarp was detected just a few meters from an MRNR forestry (Casale S. Antonio). The crown zone is associated with several minor scarps, mainly placed on the left side of the main one. A landslide terrace in the middle-high part of the SGTA body is one of the most evident landmarks. It is characterized by a widespread vegetation cover, dragged, and twisted from the detachment zone (Appendix 7a). The terrace represents a threshold that has favoured the creation of a large ephemeral pool, also helped by the impermeability of the substrate (Appendix 7a, 7b). The downvalley terrace border is delimited by a wide secondary slope. Minor scarps and steps are identified along the entire landslide body, which appears extremely heterogeneous in morphology, slope, and deposit grain sizes. Other ephemeral pools were detected, due to closed depressions caused by the blockage of original runoff paths, along the entire landslide extension and mainly near the landslide foot. Here the slope decreases drastically with local counterscarps due to the debris accumulation, giving rise to a vast wetland area, dominated by more hydrophilic species such as *Phragmites australis*, and *Arundo plinii*. The debris-earth flow morphology characterizes the half-bottom part of the landslide, with clasts of up to metric dimensions (Appendix 7c). Numerous fracturing systems are found along the entire landslide body, especially at the lateral margins where transverse cracks are frequent, in relation to lateral shear stresses.

Gullies related to the runoff water erosion are found along the entire landslide body. These are frequent in the crown area, with depths of one-meter order and lengths up to 30 meters, evolving from embryonic run-off forms (Rills, Appendix 7a). Much larger and with regressive erosion character, gullies develop from the landslide accumulation zone at the confluence with the Paglia River, flowing and delimiting the SGTA edges and joining in a single creek near the landslide toe (Fig. 4a, Appendix 8). Ephemeral and small-sized earth pyramids were found as results of the splash and sheet erosion combination (Appendix 7d). A meandering morphology was detected for the Paglia River section downslope of the SGTA, where the river follows the SW-NE direction (Fig. 4a, b1, b2). Here, the vegetation physiognomy and the topography indicate a raised area nearby the river and a trench area immediately upstream, in a "saddle" where the vegetation cover is less dense (Fig. 4a).

3.2.2 Landslide dynamic monitoring results

Considering the theoretical position error of 3 metres for sampling, among the 22

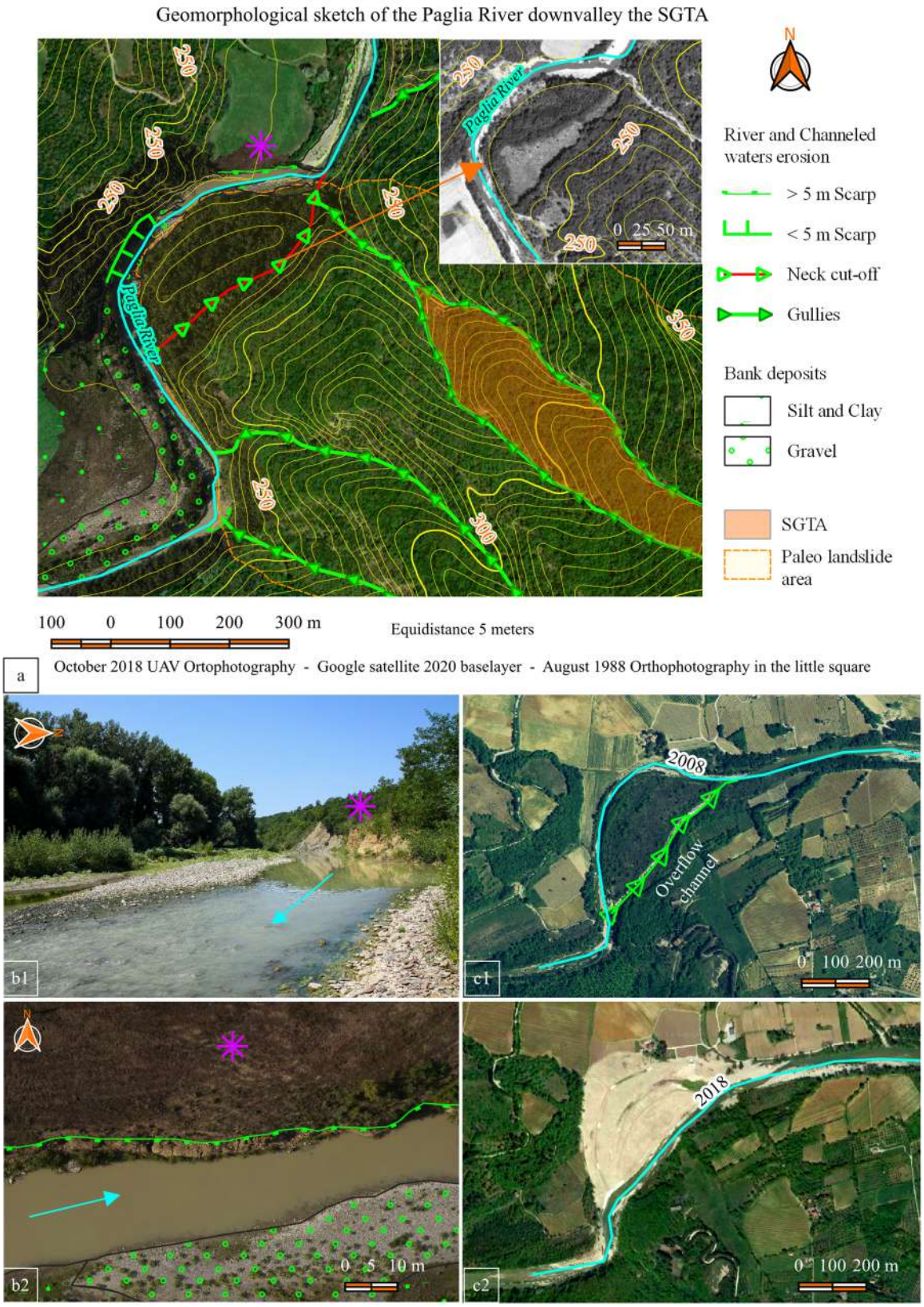

Fig. 4 Geomorphological sketch of the Paglia River downvalley the SGTA (a); Paglia River zone, note the erosional scarp on the hydrographic left (pink star in a, b1, b2) and the gravel deposits zone on the hydrographic right (b1, b2). Paglia River 10 km downvalley the SGTA, where a meander cut-off occurred between 2008 and 2018 (c1, c2).

Fig. 5 Pins with the largest displacements in the observed period. (a) Detachment niche zone near Casale S. Antonio. (b) Highest displacement zone, located downvalley of the landslide terrace.

monitoring pins, not all pins showed significant displacements during the field monitoring campaigns. The displacements are mainly directed toward the maximum slope direction (from NW to W, Fig. 5a, 5b; Fig. 6b). Displacement values are summarized in Tab.1. Among the recorded positions between November 2015 and March 2016, pin E, located about 150 meters downstream of the landslide terrace, shows 7 meters of displacement, in the N-NW direction. The most significant pins displacement occurred between March 2016 and October 2017 with a clear prevalence in the medium-high landslide portion, just downstream of the terrace. Pin 2 moves by 7.6 meters in the W direction, pin D by approximately 17 m in the W direction, pin 3 by approximately 14 m in the NW direction, pin E by 6.7 m in the W-SW direction, pin 4 by 8.5 m in the direction NW. Pin C moves 5 meters in the NW direction.

As regards 2018, no values exceed the 6 meters threshold. However, between May 2018 and July 2018, pin D shows a 5.7 meters displacement in the W direction, a value which, although below the threshold,

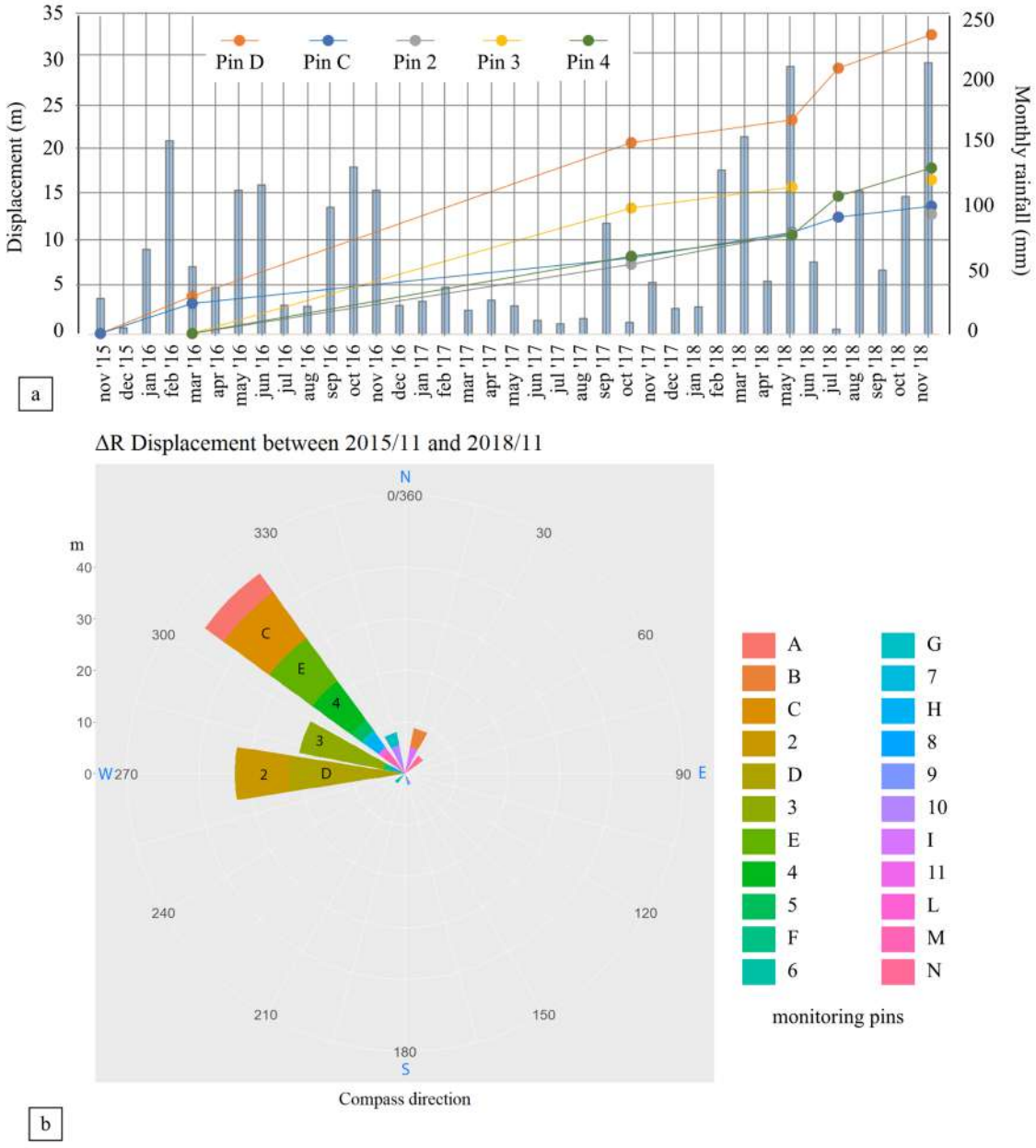

Fig. 6 Comparison between precipitation trend and total displacements (Δm) of the pins D, C, 2, 3, 4 (a); Displacement magnitude and direction between the first and the last sampling ΔR: 2015-2018 (b).

Table 1 Pins monitoring complete results. Δm: displacement (meters) between two successive reliefs; Values in bold: displacement > 6 meters; Values is underlined: displacement near 6 meters. ΔR shows the displacement between the first and last pin position and the relative mean speeds. Note that pin 1 has been lost during the monitoring period.

Pin 11/'15	Δm 03/'16	Δm 10/'17	Δm 05/'18	Δm 07/'18	Δm 11/'18	Δm total	ΔR 11/'15, 11/'18	Mean speed (cm/day)
A	4.8 NNE	4.4 WSW	1.4 NW	1.3 SW	1.3 ENE	13	4.5 NW	0.41
B	0.9 NW	4.2 WSW	4.7 ENE	3.5 NW	1.7 NE	15	3.8 NNE	0.35
C	3.3 WNW	5 NW	2.8 NW	1.7 W	1.2 SE	14	**11 NW**	1.00
2	/	**7.6 W**	3.4WNW	/	2.1 SSE	13.1	**10.5 W**	0.99
D	4.1 W	**16.9 W**	2.5 N	5.7 W	3.7 ESE	33	**22.5 W**	2.11
3	/	**13.8WNW**	2.3 W	/	0.8 NW	16.9	**16.7WNW**	1.57
E	**7.02NNW**	**6.7 WSW**	2.6 SW	2.4NW	2.1 NW	20.9	**10. 3 NW**	0.97
4	/	**8.5 NW**	2.3 NE	4.3 W	3.1 W	18.2	**9.3 NW**	0.87
5	/	/	3.6 N	/	2 NW	5.6	2.5 NW	0.23
F	0.9 NW	2.2 N	0.6 NNE	0.4SW	2.9 SSE	7	1.5 WNW	0.14
6	/	1.7 NW	2.2 SW	/	2.6 SE	6.5	2.4 SW	0.23
G	0.7 ENE	1.6 N	1.8 NW	0.3 ESE	0.4 SSE	4.6	2.5 NNW	0.24
7	/	2.6 NNW	1.5 SSW	/	0.7 SW	4.7	0.9 NW	0.08
H	3.9 N	2.8 SSE	/	1.2 S	3.8 NW	11.7	3.1 NW	0.29
8	/	1.4 NNE	/	/	3.4 SW	4.8	2.7 WSW	0.25
9	/	3.0 WSW	/	2 SSW	2.8 ENE	7.8	2.3 SSE	0.22
10	/	2.7 NW	/	/	3.16NNW	5.8	5.7NNW	0.54
I	5.4 NE	1.2 WSW	/	1.3WSW	0.6 NW	8.4	3.7 NNE	0.35
11	/	1.6 NE	/	2.9NNW	3.1 SSW	7.6	1 NW	0.09
L	2.8 SE	3.7 NNE	/	/	3.9 W	9.4	1.5 NNE	0.14
M	2.2 NNW	1.9 NE	/	/	2.9 W	7.3	5.4 NW	0.51
N	4.3 NE	/	/	/	/	4.3	4.3 NE	0.40

is very close to the latter and consistent with the general displacement trend (Fig. 5b, Table 1).

Finally, from the resulting shift (ΔR) between the first sampled position (November 2015) and the last (November 2018), the displacement patterns in Tab. 1 can be deduced. For this purpose, the displacement observed in the mid portion of the landslide body, represented by a total displacement of 22.5 m for pin D, is confirmed by the photointerpretation using Google Earth historical view function. Here, indeed, a displacement of above 23 m was measured between the consecutive positions of a touristic panel in the same time interval.

The comparison between the landslide dynamic monitoring and the precipitation trend shows a general correspondence between the major displacement and the precipitation peaks, that correspond to or anticipate the observed displacement as shown in Fig 6a. In particular, during the late spring of 2018, the greatest pin displacement rate was measured (up to 5.7 meters in only two months, Pin D), which can be associated with the high-intensity rainfall that occurred during the February- May 2018 time interval. A huge displacement was measured during the March 2016-October 2017 time interval (up to 17 meters), coinciding with a generalized deterioration of the slope stability.

4 Discussions

4.1 The SGTA morphoevolution

The collected data allowed to propose stimulating theories on the SGTA and relative landscape evolution. From the aerial photos interpretation and morphological field surveys, it can be hypothesized that the SGTA would not be the result of an isolated landslide event, but the effect of consecutive reactivations of a much larger landslide complex whose historical memory has been lost (i.e., paleo-landslide complex). A wide landslide complex might have influenced the slope evolution and even the same course of the Paglia River. The "paleo-landslide" deposits, testified by the large convex area near the valley floor on the right riverbank, could be the same responsible for the river deviation and its meandering pattern in the study area. The regressive erosion featuring gullies could represent a further sign of the "rejuvenate" effect on the relief due to the landslide deposits. The elevation trend near the Paglia River and the less dense vegetation cover could indicate gravity-related relaxation effects on the landslide deposits

combined with flood events and a "neck cut-off" (Fig. 4a). The neck cut-off is a phenomenon already observed within the catchment area (Fig. 4c1, c2), however in the SGTA complex area, could be interpreted as a flow adaptation of the Paglia, in response of gravitational relaxations in the paleo-landslide deposits. This would be supported by the current morphology considering that the river, near the meander, is forced to the hydrographic left by a steeper slope under lateral erosion (Fig. 4a, b1, b2; Appendix 8c). The asymmetry in the valley shape so could find an explanation in the landslide complex effects on the hydrographic right and on the river adjustments to reach the new equilibrium.

A final consideration concerns the gully erosion processes near the landslide head. These could indicate a temporary prevalence of run-off water erosive phenomena on the clays disturbed by the landslide action (Appendix 7a). This trend is also supported by the erosion measurements carried out in previous geomorphological surveys (Aleotti, Fontana e Sacchetti 2016) It shows the maximum erosion values in the crowning area, whereas the present study monitoring shows the lowest displacements recorded. The gullies' presence may also be a manifestation of the piping phenomenon, the aqueduct leaks and the fractured clays' predisposition to rainwater infiltration. The piping hypothesis is strengthened by the widespread transverse and longitudinal cracks that are found along the entire landslide body and in the trees aspect in the crowning zone. These show various and inconsistent stem inclinations, like those found in previous studies for neighbouring geological contexts such as the Orcia River catchment in Southern Tuscany (Bollati et al. 2012).

Concerning the SGTA dynamic monitoring, since 2015, a general state of activity is observed. The greater displacement is detected in the medium-high portion of the landslide body, immediately downvalley of the landslide terrace (Fig. 3a, d; Fig. 5a; Fig. 6a) and reaches considerable values in the first monitoring period 2016-2017, up to 17 meters and up to mean speed of 2.9 cm/day. In particular, the observed displacements, between November 2015 and March 2016, could be related to the high February precipitations, which followed a relatively arid period. Similarly, the greatest displacement, observed in the March 2016-October 2017, and May-July 2018 time intervals, could be related to alternating arid-rainy precipitation patterns.

4.2 From landslide management to enhancement of the SGTA as an element of the geoheritage in the MNRM

The application of a well-tested and simple LSA method, based on conditional analysis and unbiased selection of triggering factors, allowed a reproducible workflow for the management tasks of the nature reserve. 30.3% of the MRNR extent resulted in the landslide-prone area (in the susceptibility classes 4 and 5), due to the effect of the combination of peculiar environmental features. This condition may represent a source of risk for people and infrastructures in the area. On the other side, it may represent also an opportunity for education of people to hazards due to gravity- and water-related processes (Coratza and De Waele 2012). Indeed, the SGTA may be considered a geoheritage element concerning its scientific, cultural and ecological values (Bollati et al. 2017a). Like other gravity-related landforms (Bollati et al. 2017b), SGTA has left impressive marks on the landscape, and it may be considered in the specific geomorphosite (Panizza 2001).

According to the classification by Pelfini & Bollati (2014), this is a case of active geomorphosites, where genetic processes are still active, assuming a high educational value (e.g., Reynard et al. 2007). Another exemplary active geomorphosite in Central Italy is the "Calanchi di Civita di Bagnoregio". This is the case of a typical badlands landscape, characterized by a geological and morphological setting similar to the MRNR one, highly prone to gravity- and washout processes (Cresta 2005), and where gravity processes are deeply conditioned by the high rheological contrast between the volcanic cap rocks, where villages are built, and the underlying clay rocks (Del Monte 2017; Amici et al. 2017). Landslides, surely represent examples of active geomorphosites, standing out for their scientific value, for their impressive impact on the landscape (i.e., profound scars; in some cases very scenic), and for the implication, they could have for valorization and fruition dissemination of the geomorphosites (Niculiţă and Mărgărint 2018). They have been defined in literature also as "moving Geosite" (Calcaterra et al. 2014) with a fundamental role in geoparks enhancement. In this framework, the SGTA represents an active-moving geomorphosite due to its dynamism, testified by the performed GPS monitoring, representing a valuable resource for natural reserve enhancement.

Concerning more in detail its value as

geomorphosite, the ecologic support role (Bollati et al. 2017a) (see, ephemeral pools, and renewal of the vegetation series as an example) is evident, as demonstrated in other studies (Bollati et al. 2012; Forno et al. 2022). These values acquire a particular significance in the context of a protected area where knowledge of the natural heritage lays the foundations for environmental protection (Zgłobicki et al. 2017, 2018). From this point of view, the MRNR represented a virtuous example of promotion, since already in 2005 a geotouristic itinerary was implemented to allow educational knowledge about the landslide (see the trail "La Scialimata" in Appendix 8 Trail path network susceptibility analysis). But the trail was damaged after one of the landslide's greatest displacements, and then not refurbished (examples of the trail damages are visible in a photo of attachment Appendix 8).

The MRNR indeed is characterized by evocative toponyms such as "Scialimata" or "lama" that reflect the landslide's influence on cultural development. The SGTA toponym itself represents the coevolution between territorial peculiarities and linguistic ones, with which the populations refer to natural objects. This increases the cultural value of this landslide, as already occurred in other cases in Italy (Civita di Bagnoregio) and abroad (e.g., Niculiţă and Mărgărint 2018).

The SGTA, as active geomorphosites, offers the rare opportunity to monitor and observe the geomorphological processes in a context of an open-air laboratory, as mentioned before, increasing its educational value (Reynard et al. 2007; Pelfini et al. 2016, 2019). This confers to the sites, if carefully and safety-oriented managed, to be a tool for raising awareness in Society about hydrogeological instabilities affecting the Italian territory (Coratza and De Waele 2012). According to the VISIG - Intrinsic Value of the Geological Site of Interest, the methodology adopted for the quali-quantitative classification of the geosites, used in the Lazio Region Geosite database (Direzione Regionale Capitale Naturale 2015), the SGTA is classified in the middle class of interest. This index consists of the weighted summary of three different values: representativeness (RP), rarity (RR) and aesthetic-scenic value (SE). It should be important to reconsider its assessment considering other values like the ecological support role and the educational value, as described above. Moreover, the geosite is absent from the Italian Geosite Inventory (ISPRA 2009), and it should be considered for insertion in the national list.

For all these reasons, slope stability management should be enhanced within the reserve, to effectively mitigate landslide hazards and propose sustainable forms for geoheritage enhancement. The road network (Appendix 5) and the trail network (Appendix 6) susceptibility maps allowed us to identify the most dangerous areas in terms of landslide susceptibility (Fig. 7), they represent an instrument for decision-makers to evaluate and mitigate the deriving risks. For this purpose, attention should be posed by the reserve managers on the road traits characterized by the highest susceptibility classes, and by a high frequentation. Moreover, some trails such as the "Sentiero dei Briganti", and "Sentiero natura Felceto" in the northern MRNR and the "Sentiero del Fiore" in the southern MRNR are characterized by traits classified as highly susceptible, despite being classified as touristic in terms of difficulty. Even the hiking trail on the SGTA "La Scialiamata", already damaged in 2010, presents high susceptibility traits (Appendix 6). This should be considered in the touristic paths planning, or in the risk mitigation actions, such as information panels on landslide risks, or promoting thematic seminars for tourists and hikers.

5 Conclusions and Future Perspectives

The research aimed to investigate the SGTA landslide as an element of the geoheritage in the MRNR nature reserve management. It is featured by scientific, cultural and ecological value, but it may also represent an element of potential risk. A multi-scalar approach was applied, to analyse the landslide features, in terms of distributions and effects, starting from the MRNR scale to the single landslide local scale (i.e., SGTA). For this, the SGTA landslide was chosen as a representative landslide of the reserve, both in terms of landslide feature and dynamic and in terms of nature conservancy and management as a geoheritage element, being an active geosite.

At the MRNR scale, the Landslide Susceptibility Analysis represents a useful tool for land use spatial planning and decision-making. In this study, the best LSA resulted from the combination of Slope, Curvature and Drainage density factors, which better explains the landslide distribution in the reserve. The road network and the trail network susceptibility maps allowed us to identify the most dangerous areas in terms of landslide

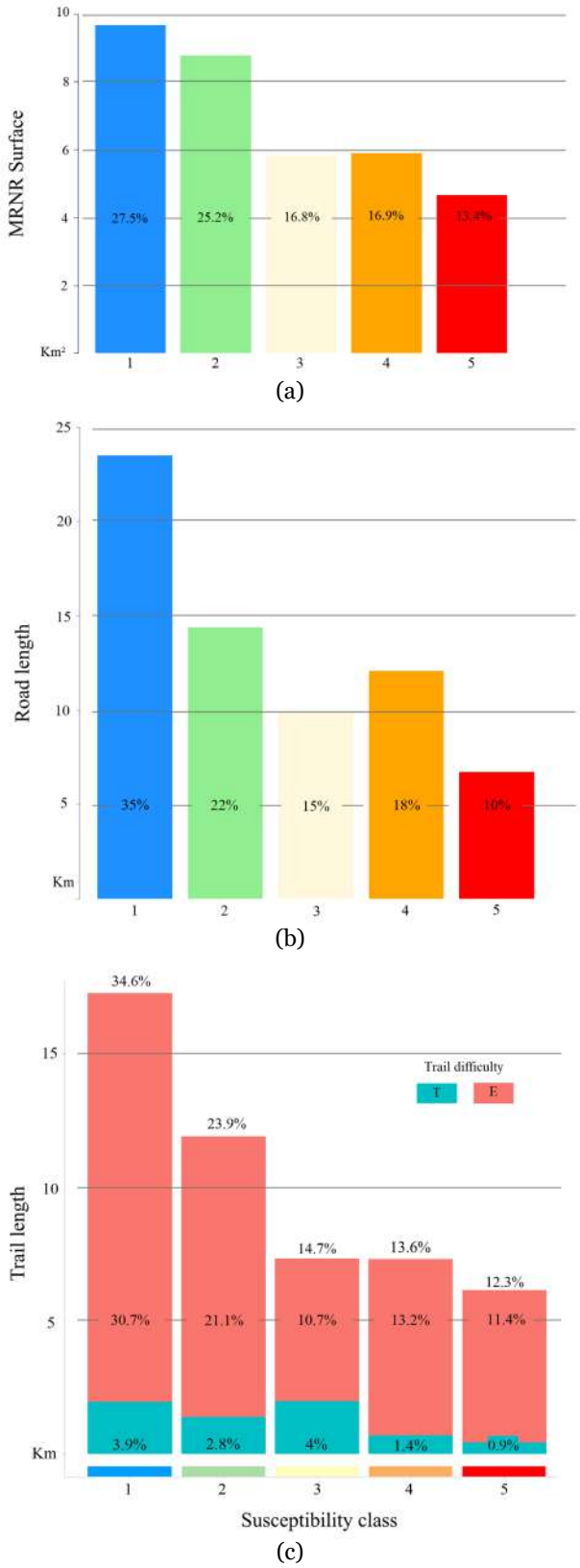

Fig. 7 Landslide susceptibility scores. (a) MRNR area for each susceptibility class; (b) Intersect scores between the LSA and the Road; (c) Intersect scores between the LSA and the Trail Network.

susceptibility, and to evaluate and mitigate the deriving risks, planning consequently the touristic offer. For this purpose, attention should be paid to the road traits characterized by the highest susceptibility classes, and by a high frequentation. Indeed, some trails are characterized by traits classified as highly susceptible, despite being classified as touristic in terms of difficulty. This should be considered in the touristic paths planning, or for the risk mitigation actions, such as information panels, or thematic seminars on hazards in a landslide-prone environment.

As regards the SGTA scale this study allowed us to identify the activity status of the landslide, highlighting its dynamic features, and making some interesting hypotheses on its evolution in the framework of the MRNR landscape evolution. The SGTA could represents the last effect of an imponent landslide complex, that might have influenced the entire slope evolution and the Paglia River valley aspect, through a river deviation that results in the actual meandering pattern. The SGTA monitoring allowed us to classify the process as active, where the greatest displacement is detected in the medium-high portion of the landslide body until values of up to 17 meters in the period of major activity between 2016 and 2017. The displacements seem related to a well-known precipitation pattern, where a vast period of relative drought followed by a very rainy one favour runoff and gravity-related processes. In this case, a precise relationship between the observed displacements and the rainfall trend is masked by other factors such as the effects of leaks in the public pipelines, that could favour the piping effects in clays substrates.

Taking into account the possible risks derived from the SGTA's active status, it surely represents an opportunity for geotourism, geo-education (Bollati et al. 2012) and, also for stakeholders for example for testing visitors (Garavaglia et al. 2012). Nevertheless, under dynamic conditions, trails can be impacted by mass transport as happened to the touristic trail "La Scialimata", which underwent disruption by the landslide activity in 2010 and today already presents traits characterized by a high landslide susceptibility (Appendix 8). For this reason, adequate management strategies are important, considering both the educational value and safety issues (Brandolini and Pelfini 2010) and the monitoring activity is still considered a priority. The UAV *sfm* technique indeed has proved to be an extremely effective, quick, and relatively cheap tool in the acquisition of spatial

landslide information in this study, and could be considered a tool for monitoring this active-moving geosite, becoming a potential tool for "equipping" an SGTA open-air laboratory. New UAV surveys, could allow us to evaluate, through the Difference of DEM technique, or by point clouds comparisons, the morphological variations that occurred in the analysed time interval (Betz et al. 2019).

In conclusion, this study put the first steps in the management of landslides in the nature reserves frameworks, considering both their features as potential risks, that surely must be considered in the land use planning, but also as hot spots of geoheritage, where it is possible to directly observe the effects of these processes on landscapes and ecosystems. The use of a multi-scalar approach highlights the potentiality of connecting the regional spatial scale to the local one, intending to complete the knowledge of these phenomena. Moreover, this study prompts us to reconsider the SGTA classification considering values not yet considered in the assessment process, such as the ecologic support role and the educational value, and the necessity of integrating the regional geosites lists with the national one, where the SGTA has not yet been listed.

Acknowledgments

The authors thank the Monte Rufeno Nature Reserve staff for the scientific and logistic support and the NHAZCA S.r.l. for contributing to the UAV operations. A special thanks to the anonymous reviewers for their valuable contributions to the improvement of this work.

Electronic supplementary material: Supplementary material (Appendixes 1-8) is available in the online version of this article at https://doi.org/10.1007/s11629-022-7596-y.

Open Access funding provided by Università degli Studi di Milano within the CRUI-CARE Agreement.

References

Aleotti L, Fontana F, Sacchetti N (2016) Hydrogeological report on the "Scialimata Grande di Torre Alfina" landslide. Technical hydrogeological report. La Sapienza University, IT. (In Italian)

Amici V, Maccherini S, Santi E, et al. (2017) Long-term patterns of change in a vanishing cultural landscape: a GIS-based assessment. Ecolog Informat 37: 38-51. https://doi.org/10.1016/j.ecoinf.2016.11.008

Amodio M, De Rita D, Di Filippo M, et al. (1987) Geological-structural evolution of the Bolsena volcano-tectonic (vulsino volcanic complex). Bollett Grup Naz Vulcan 21 - 36.

Arsial (2021) Agrometeorological integrated services. http://www.arsial.it/portalearsial/agrometeo/F1.asp

Ayalew L, Yamagishi H (2005) The application of GIS-based logistic regression for landslide susceptibility mapping in the Kakuda-Yahiko Mountains. Central Japan. Geomorphology 65: 15-31. https://doi.org/10.1016/j.geomorph.2004.06.010

Belisario F (2003) Geosite n°396. Geosites database of the Lazio region. (In Italian). https://dati.lazio.it/catalog/it/dataset/banca-dati-dei-geositi-del-lazio

Belisario F, Romagnoli C (2010) Report on the damage to the natural-engineering works of the hiking trail "La Scialimata" (Monte Rufeno nature reserve) caused by the exceptional rainfall of November 2010. MRNR Technical Reports. (In Italian)

Bertolini G, Corsini A, Tellini G (2017) Fingerprints of large-scale landslides in the landscape of the Emilia Apennines. In: Soldati M. and Marchetti M (eds.), Landscapes and Landforms of Italy. World Geomorphological Landscapes. Springer, Cham. pp 215-224. https://doi.org/10.1007/978-3-319-26194-2_18

Betz S, Croce V, Becht M (2019) Investigating morphodynamics on Little Ice Age lateral moraines in the Italian Alps using archival aerial photogrammetry and airborne LiDAR data. Zeit für Geomorph 62(3): 231-247. https://doi.org/10.1127/zfg/2019/0629

Blasi C (1993) Phytoclimatic map of the Lazio region. Reg Lazio, Univ La Sapienza, Dip Biolog Veg, IT. (In Italian)

Bolia P, La Vecchia G, Giaquinto S, et al. (1982) Geological-

structural features of the Paglia river catchment. In: Bacino del Fiume Paglia: Studi Strutturali, Idrogeologici, Geochimici. CNR, PFE, RF 16. (in Italian)
Bollati I, Coratza P, Panizza V, Pelfini M (2018) Lithological and structural control on Italian mountain geoheritage: opportunities for tourism, outdoor and educational activities. Quaest Geog 37(3): 53-73. https://doi.org/10.2478/quageo-2018-0025
Bollati I, Crosa Lenz B, Zanoletti E, Pelfini M (2017a) Geomorphological mapping for the valorization of the alpine environment. A methodological proposal tested in the Loana Valley (Sesia Val Grande Geopark, Western Italian Alps). J Mt Sci 14(6): 1023 - 1038. https://doi.org/10.1007/s11629-017-4427-7
Bollati I, Della Seta M, Pelfini M, et al. (2012) Dendrochronological and geomorphological investigations to assess water erosion and mass wasting processes in the Appennines of Southern Tuscany (Italy). Catena 90: 1-17. https://doi.org/10.1016/j.catena.2011.11.005
Bollati I, Pellegrini M, Reynard E, Pelfini M (2017b) Water driven processes and landforms evolution rates in mountain geomorphosites: example from Swiss Alps. Catena 158: 321-339. https://doi.org/10.1016/j.catena.2017.07.013
Bollati I, Smiraglia C, Pelfini M (2013) Assessment and Selection of Geomorphosites and Trails in the Miage Glacier Area (Western Italian Alps). Env Manag 51(4): 951-967. https://doi.org/10.1007/s00267-012-9995-2
Bollati I, Vergari F, Del Monte M, Pelfini M (2016) Multitemporal dendrogeomorphological analysis of slope instability in upper Orcia Valley (Southern Tuscany, Italy). Geog Fis Din Quat 39(2): 105-120. https://doi.org/10.4461/%20GFDQ%202016.39.10
Brandolini P, Faccini F, Pelfini M, Firpo M (2013) A complex landslide along the Eastern Liguria rocky coast (Italy). Rend on Soc Geol It 28: 28-31. https://hdl.handle.net/2434/234508
Brandolini P, Pelfini M (2010) Mapping geomorphological hazard in relation to geotourism and hiking trails. In: Regolini-Bissing G, Reynard E (eds.), Mapping Geoheritage, Lausanne, Institut de géographie, Géovision: 35: 31-45. https://hdl.handle.net/2434/151693
Calcaterra D, Guida D, Budetta P, et al. (2014) Moving geosites: how landslides can become focal points in Geoparks. In: Latest Trends in Engineering, Mechanics, Structures, Engineering Geology. Salerno, Italy: 162-171.
Campobasso C, Carton A, Chelli A, et al. (2018) Geomorphological map of Italy 1:50.000. New guidelines and integrations. In: ISPRA, Servizio Geologico d'Italia. Progetto CARG: Modifiche ed Integrazioni al Quaderno N. 4/1994. (In Italian)
Carrara A, Cardinali M, Guzzetti F, Reichenbach P (1995) GIS technology in mapping landslide hazard. In: Carrara A, Guzzetti F (eds.), Geographical Information Systems in Assessing Natural Hazards. Kluwer, Dordrecht 135-175. https://doi.org/10.1007/978-94-015-8404-3_8
Chung CF, Fabbri A (2003) Validation of spatial prediction models for landslide hazard mapping Nat Hazards 30: 451-472. https://doi.org/10.1023/B:NHAZ.0000007172.62651.2b
Ciccacci S, D'Alessandro L, Fredi P, Lupia Palmieri EN (1998) Geomorphic-quantitative analyses contribute to the denudation processes of the Paglia river catchment. Torino: Supp Geog Fis Din Quat– Supp. I - Comitato glaciologico italiano. (In Italian)
Ciotoli G, Della Seta M, Del Monte M, et al. (2003) Morphological and geochemical evidence of neotectonics in the volcanic area of Monti Vulsini (Latium, Italy). Quat Intern 101-102: 103-113. https://doi.org/10.1016/S1040-6182(02)00093-9
Clerici A, Tellini C, Vescovi P (2006) Landslide failure and runout susceptibility in the upper T. Ceno valley (Northern Apennines, Italy). Nat Haz. https://doi.org/10.1007%2Fs11069-009-9349-4
Coratza P, De Waele J (2012) Geomorphosites and natural hazards: teaching the importance of geomorphology in society. Geoheritage 4(3): 195-203. https://doi.org/10.1007/s12371-012-0058-0
Cresta S, Fattori C, Mancinella D, Basilici S (2005) Lazio geodiversity – Geosites and geoconservation in the system of protected areas. ARP - Regione Lazio.
Dailling JW (1994) Vegetation Colonization of Landslides in the Blue Mountain, Jamaica. Biotropica: 392 - 399. https://doi.org/10.2307/2389233
Damiani AV (1991) Stratigraphic-structural observations on the valleys of Paglia and Tevere rivers. Stud Geol Camerti, Spec 1:243-250. (In Italian). http://193.204.8.201:8080/jspui/handle/1336/560
Damiani AV, Mencarelli I (1991) Structural controls on the etruscan deposits in the tectonic window of Monte Peglia. Rend Soc Geol Ital 13:147-150. (In Italian)
Della Seta M, Del Monte M, Fredi P, Lupia Palmieri E N (2009) Space-time variability of denudation rates at the catchment and hillslope scales on Thyrrenian side of Central Italy. Geomorphology 107(3-4):161-177. https://doi.org/10.1016/j.geomorph.2008.12.004
Del Monte M (2017) The typical badland landscapes between the Tyrrhenian Sea and the Tiber River. In: Soldati M, Marchetti M (eds.), Landscapes and Landforms of Italy. Springer, Cham. pp 281-291. https://doi.org/10.1007/978-3-319-26194-2
Diéz-Herrero A, Vegas J, Carcavilla L, et al. (2018) Techniques for the monitoring of geosites in Cabañeros National Park, Spain. Geoheritage 417-430. https://doi.org/10.1016/B978-0-12-809531-7.00024-1
Direzione Regionale Capitale Naturale, Parchi e Aree Protette (2015) Web repository of the Lazio Region Geosites. (In Italian). http://dati.lazio.it/catalog/it/dataset/banca-dati-dei-geositi-del-lazio
Fantucci R, McCord A (1995) Reconstruction of landslide dynamic with dendrochronological methods. Dendrochronologia 13: 43-58.
Fredi P, Ciccacci S (2017) A Route of Fire in Central Italy: The Latium Ancient Volcanoes. In: Soldati M and Marchetti M (eds.), Landscapes and Landforms of Italy. World Geomorphological Landscapes. Springer, Cham: 303-315 https://doi.org/10.1007/978-3-319-26194-2_26
Fredi P, Lupia Palmieri E N (2017) Morphological Regions of Italy. In: Soldati M and Marchetti M (eds.), Landscapes and Landforms of Italy. World Geomorphological Landscapes. Springer, Cham: 39-74 https://doi.org/10.1007/978-3-319-26194-2_5
Forno MG, Gianotti F, Gattiglio M, et al. (2022) How Can a Complex Geosite Be Enhanced? A Landscape-Scale Approach to the Deep-Seated Gravitational Slope Deformation of Pointe Leysser (Aosta Valley, NW Italy). Geoheritage 14(3): 1-33. https://doi.org/10.1007/s12371-022-00730-8
Fugazza D, Scaioni M, Corti M, et al. (2018) Combination of UAV and terrestrial photogrammetry to assess rapid glacier evolution and map glacier hazards. Nat Hazards Earth Syst Sci 18: 1055-1071. https://doi.org/10.5194/nhess-18-1055-2018
Garavaglia V, Diolaiuti G, Smiraglia C, et al. (2012) Evaluating Tourist Perception of Environmental Changes as a Contribution to Managing Natural Resources in Glacierized Areas: A Case Study of the Forni Glacier (Stelvio National Park, Italian Alps). Env Manag 50(6): 1125 - 1138. https://doi.org/10.1007/s00267-012-9948-9
Garavaglia V, Pelfini M, Bini A, et al. (2009) Recent evolution of debris-flow fans in the Central Swiss Alps and associated risk assessment: two examples in Roseg Valley. Phys Geography 30(2): 105-129 https://doi.org/10.2747/0272-3646.30.2.105
Guida D, Pelfini M, Santilli M (2008) Geomorphological and dendrochronological analyses of a complex landslide in the Southern Apennines. Geografiska Annaler: Series A, Phys Geography: 211-226. https://doi.org/10.1111/j.1468-0459.2008.340.x
Hutchinson MF, Dowling TI (1991) A continental hydrological assessment of a new grid-based digital elevation model of

Australia. Hydrol Proc 5: 45-58. https://doi.org/10.1002/hyp.3360050105
IFFI (2007) Landslides National Inventory of Italy. APAT. (In Italian). https://www.isprambiente.gov.it/it/progetti/cartella-progetti-in-corso/suolo-e-territorio-1/iffi-inventario-dei-fenomeni-franosi-in-italia
ISPRA (2009) Geosites National Inventory. (In Italian). http://sgi.isprambiente.it/geositiweb/
Korup O (2005) Geomorphic imprint of landslides on alpine river systems, southwest New Zealand. Earth Surf Proc and Land 30(7): 783-800. https://doi.org/10.1002/esp.1171
Lazio Region Open Data (2003) CTR 1:5.000 - Provincia di Viterbo. (In Italian). (http://dati.lazio.it/catalog/it/dataset/carta-tecnica-regionale-2002-2003-5k-viterbo)
Leonelli G, Bollati I M, Cherubini P, et al. (2022) Tree-ring stable isotopes indicate mass wasting processes at Radicofani in the upper Orcia Valley (Tuscany, Italy). Sci of The Tot Env 812: 152428. https://doi.org/10.1016/j.scitotenv.2021.152428
Lucieer AS, De Jong M, Turner D (2014) Mapping landslide displacements using structure from motion (SfM) and image correlation of multi-temporal UAV photography. Prog in Phys Geography: 38(1): 97-116. https://doi.org/10.1177/0309133313515293
Margottini C, Melelli L, Spizzichino D (2017) The Tuff Cities: A "Living Landscape" at the Border of Volcanoes in Central Italy. In: Soldati M and Marchetti M (eds.), Landscapes and Landforms of Italy. World Geomorphological Landscapes. Springer, Cham. pp 293-301. https://doi.org/10.1007/978-3-319-26194-2_25
Martino S, Battaglia S, D'Alessandro F, et al. (2020) Earthquake-induced landslide scenarios for seismic microzonation: application to the Accumoli area (Rieti, Italy). Bull Earthquake Eng 18: 5655-5673. https://doi.org/10.1007/s10518-019-00589-1
Nagarajan R, Roy A, Vinod Kumar R, et al. (2000) Landslide hazard susceptibility mapping based on terrain and climate factors for tropical monsoon regions. Bull Eng Geol Env 275-287. https://doi.org/10.1007/s100649900032
Niculiţă M, Mărgărint MC (2018) Landslides and Fortified Settlements as Valuable Cultural Geomorphosites and Geoheritage Sites in the Moldavian Plateau, North-Eastern Romania. Geoheritage 10: 613-634. https://doi.org/10.1007/s12371-017-0261-0
Noti V (2018) GIS Open Source per Geologia e Ambiente. Dario Flaccovio Editore, Italy. (In Italian)
Panizza M (2001) Geomorphosites: concepts, methods and examples of geomorphological survey. Chi Sci Bull 4-5. https://doi.org/10.1007/BF03187227
Pelfini M, Bollati I (2014) Landforms and geomorphosites ongoing changes: Concepts and implications for geoheritage promotion. Quaest Geog 33(1): 131-143. https://doi.org/10.2478/quageo-2014-0009
Pelfini M, Bollati I, Pellegrini L, Zucali M (2016) Earth Sciences on the field: educational applications for the comprehension of landscape evolution. Rend On Soc Geol It 40: 56-66. https://doi.org/10.3301/ROL.2016.72
Pelfini M, Parravicini P, Fumagalli P, et al. (2019) New methodologies and technologies in Earth Sciences education: Opportunities and criticisms for future teachers. Rend Online Soc Geol It 49: 4-10. https://doi.org/10.3301/ROL.2019.45
Pelfini M, Santilli M (2008) Frequency of debris flows and their relation with precipitation: A case study in the Central Alps, https://doi.org/10.1016/B978-0-12-813054-4.00009-5
Italy. Geomorphology 101: 721-730. https://doi.org/10.1016/j.geomorph.2008.04.002
Ramsankaran RP, Navinkumar J, Kulkarni AV (2021) UAV-based Survey of Glaciers in Himalayas: Challenges and Reccomendations. J Indian Soc Remote Sens 49: 1171-1187. https://doi.org/10.1007/s12524-020-01300-7
Remondo J, Gonzales A, Diaz De Teràn JR, et al. (2003) Validation of landslide susceptibility maps; examples and applications from a case study in Northern Spain. Nat Hazards 30: 437-449. https://doi.org/10.1023/B:NHAZ.0000007201.80743.fc
Reynard E, Fontana G, Kozlik L, Scapozza C (2007) A method for assessing scientific and additional values of geomorphosites. Geog. Helvetica 62(3): 148-158. https://doi.org/10.5194/gh-62-148-2007
Rossi G, Tanteri L, Tofani V, et al. (2018) Multitemporal UAV surveys for landslide mapping and characterization. Landslides - ICL/IPL Activities. https://doi.org/10.1007/s10346-018-0978-0
Santacana N, Baeza B, Corominas J, et al. (2003) A GIS-based multivariate statistical analysis for shallow landslide susceptibility mapping in La Pobla de Lillet Area (Eastern Pyrenees, Spain). Nat Hazards 30: 281-295. https://doi.org/10.1023/B:NHAZ.0000007169.28860.80
Shiels B, Walker LR (2013) Landslides cause spatial and temporal gradients at multiple scales in the Luquillo Mountains of Puerto Rico. USDA National Wildlife Research Center - Staff Publications 1581.
Stark M, Neugirg F, Kaiser A, Della Seta M (2020) Calanchi badlands reconstructions and long-term change detection analysis from historical aerial and UAS image processing. J Geomorph. https://doi.org/10.1127/jgeomorphology/2020/0658
Sterlacchini S, Ballabio C, Blahut J, et al. (2011) Spatial agreement of predicted patterns in landslide susceptibility maps. Geomorphology 125: 51-61. https://doi.org/10.1016/j.geomorph.2010.09.004
Vergari F (2015) Assessing soil erosion hazard in a key badland area of Central Italy. Nat Haz 79: S71-S95. https://doi.org/10.1007/s11069-015-1976-3
Vergari F, Della Seta M, Del Monte M, et al. (2011) Landslide susceptibility assessment in the Upper Orcia Valley (Southern Tuscany, Italy) through conditional analysis: a contribution to the unbiased selection of causal factors. Nat Hazards Earth Syst Sci 11: 1475-1497. https://doi.org/10.5194/nhess-11-1475-2011
Vergari F, Troiani F, Faulkner H P, et al. (2019) The use of the slope–area function to analyse process domains in complex badland landscapes. Earth Surf. Proc. and Landforms 44(1): 273-286. https://doi.org/10.1002/esp.4496
Yeh F, Huang C, Han J, Ge L (2017) Modelling slope topography using unmanned aerial vehicle image technique. 10617 Taipei, Taiwan: Dep of Civil Eng, National Taiwan University, MATEC Web of Conference 147: 07002. https://doi.org/10.1051/matecconf/201814707002
Zgłobicki W, Poesen J, Cohen M, et al. (2017) The potential of permanent gullies in Europe as geomorphosites. Geoheritage: 1-23.https://doi.org/10.1007/s12371-017-0252-1
Zgłobicki, W, Poesen, J, Daniels, M, et al. (2018). Geotouristic value of Badlands. In: Badlands Dynamics in a Context of Global Change. Elsevier. pp 277-313.